THE JOURNAL OF PHYSICAL CHEMISTRY B

ARTICLE

pubs.acs.org/JPCB

Intracellular pH Sensing Using Autofluorescence Lifetime Microscopy

Shinya Ogikubo,[†,‡] Takakazu Nakabayashi,[†] Takashi Adachi,[‡] Md. Serajul Islam,[†] Tomokazu Yoshizawa,[†] Masataka Kinjo,[§] and Nobuhiro Ohta[*,†]

[†]Research Institute for Electronic Science, Hokkaido University, Sapporo 001-0020, Japan

[‡]Frontier Core-Technology Laboratories, FUJIFILM Corporation, Kaisei-Machi, Ashigarakami-Gun, Kanagawa 258-8577, Japan

[§]Faculty of Advanced Life Science, Hokkaido University, Sapporo 001-0021, Japan

Supporting Information

ABSTRACT: Fluorescence lifetime images of reduced nicotinamide adenine dinucleotide (NADH) that is a key cofactor in cellular metabolism were obtained in a cell at various values of intracellular pH. The average fluorescence lifetime of NADH is found to become shorter monotonically with increasing pH, indicating that pH in a single cell can be determined by fluorescence lifetime imaging of NADH without adding exogenous fluorescent probes. The magnitude of the pH-induced lifetime change is higher in cells than that in buffer solution. The fluorescence lifetime of NADH is not uniform inside a cell; the fluorescence lifetime of nuclear NADH is shorter than that of mitochondrial NADH at each pH, and the magnitude of the pH-induced change is larger in nuclei than in other areas. The local electric field effect on the fluorescence lifetime is discussed since this effect may be one of the strong possibilities for the nonuniformity of the autofluorescence lifetime of NADH in cells.

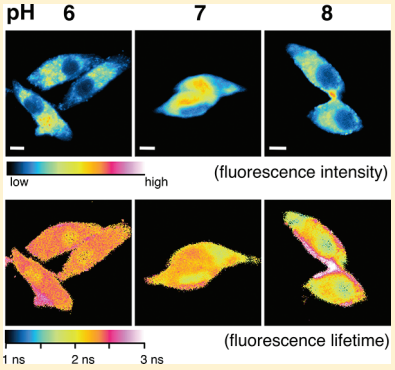

1. INTRODUCTION

Fluorescence microscopy is widely used in biochemical and biomedical research, and a variety of fluorescent dyes and proteins are now available that enable selective imaging in a single cell. In a field of diagnosis of cells and tissues, however, interest on the imaging of intrinsic fluorescence has been increasing over the past 2 decades as a noninvasive diagnostic technique.[1−7] Cells contain endogenous chromophores showing fluorescence called autofluorescence, and autofluorescence microscopy enables preservation of biological conditions without dye labeling and diagnostic tests in medicine without staining time. The well-known autofluorescent chromophores are tryptophan, porphyrin, collagen, reduced nicotinamide adenine dinucleotide (NADH), and flavins,[1,6,7] the fluorescence of which is discriminated if the proper excitation and fluorescence wavelengths are selected. These autofluorescent chromophores are related to cell functions, and measurements of autofluorescence are expected to provide a wealth of information on cellular conditions and metabolic activities.

NADH consists of nicotinamide and adenine moieties joined through their phosphate groups. NADH is known as a key cofactor for oxidation and reduction reactions and energy metabolism. NADH in the reduced form has strong absorption around 340 nm and emits blue fluorescence, which arises from the reduced form of nicotinamide. The oxidized form NAD^+, on the other hand, has an absorption band at a much shorter wavelength (∼260 nm) and exhibits no fluorescence. The fluorescence lifetime of NADH strongly depends on the environment; the fluorescence lifetime in the free state is 0.3−0.4 ns and that in the protein-bound state becomes much longer to be 2−3 ns.[3−8] It is also suggested that the fluorescence lifetime of the protein-bound NADH depends on the enzyme to which it is bound.[9] Autofluorescence of NADH is widely used to monitor intracellular environments;[1−8] however, understanding the factors governing the photoexcitation dynamics of NADH is very important for clarify physiological conditions in living systems using the autofluorescence of NADH.

In the present study, we have measured the intracellular pH dependence of the fluorescence lifetime of NADH in human cervical carcinoma (HeLa) cells. The fluorescence lifetimes of NADH are also compared in cells and in buffer solution to discuss the mechanism of their changes with medium pH. Intracellular pH is one the most important factors for understanding physiological states of cells, and significant changes in intracellular pH occur in close relationship with a variety of cellular functions such as ion transport and cell cycle.[10,11] We have shown in the present study that the intracellular pH of a single cell can be evaluated using fluorescence lifetime imaging (FLIM) of NADH. FLIM is one of the fluorescence microscopic techniques and is advantageous over intensity measurements for quantitative analyses because fluorescence lifetime is an intrinsic parameter of a chromophore, which is independent of absorption intensity, excitation light intensity, or photobleaching.[3−8,12−17] Autofluorescence lifetime imaging is therefore a promising tool for understanding intracellular environment without dye labeling.

Received: June 23, 2011
Revised: July 21, 2011
Published: July 21, 2011

dx.doi.org/10.1021/jp2058904 | J. Phys. Chem. B 2011, 115, 10385–10390

2. MATERIALS AND METHODS

A. Samples. HeLa cells were grown in a 5% CO_2 humidified atmosphere at 37 °C in Dulbecco's modified Eagle's medium (DMEM) supplemented with 10% fetal bovine serum, 1×10^5 U/L penicillin G, and 100 mg/L streptomycin sulfate for 1−2 days. Calibration of intracellular pH was performed by the so-called nigericin/high K^+ method,[18−22] in which nigericin was added to media to make equilibrium between intracellular and extracellular pH. Nigericin is an H^+ and K^+ polyether ionophore and thereby equilibrates intracellular and extracellular pH by exchanging H^+ across the plasma membrane in the presence of a depolarizing extracellular concentration of K^+. HeLa cells were rinsed once with KCl-rich media (125 mM KCl, 20 mM NaCl, 10 mM HEPES, 10 mM MES, 0.5 mM $CaCl_2$, 0.5 mM $MgCl_2$, and 13.4 uM nigericin) and then incubated with the same KCl-rich media at different pH for 15 min in a 5% CO_2 humidified atmosphere at 37 °C. The medium pH was adjusted using HCl and NaOH solutions.

B. Fluorescence Lifetime Imaging. Fluorescence lifetime images were measured using a four-channel time-gated detection system.[16,17] The second harmonic of a mode-locked Ti:sapphire laser (Spectra Physics, Tsunami) was used for excitation. The pulse duration and the repetition rate of the laser pulse were 80 fs and 81 MHz, respectively. The excitation beam was introduced into a confocal scanning microscope (Nikon, Digital Eclipse C1). The excitation beam was focused onto HeLa cells placed on the stage of the inverted microscope through the objective lens (40×), and the fluorescence emitted from the cells was collected by the same objective lens and was entered into an interference filter to select the detection wavelength of the fluorescence. The fluorescence was detected by a photomultiplier in a high-speed lifetime imaging module (Nikon Europe BV, LIMO). LIMO captures the fluorescence decay curve into four time-windows. Each reference trigger from the laser pulse train enables four time-windows sequentially, and the fluorescence photons are accumulated by one of the four time-windows. All of the time-windows were set at 2.0 ns.

C. Fluorescence Decay Profiles and Time-Resolved Fluorescence Spectra. Bulk measurements of fluorescence decay profiles as well as time-resolved fluorescence spectra of a population of HeLa cells and NADH in aqueous solution were carried out by a homemade time-correlated single-photon-counting (TCSPC) system.[23] The second harmonic of the mode-locked Ti:sapphire laser was used for excitation, and its repetition rate was reduced from 81 to 5.8 MHz using an electrooptic (EO) modulator. Fluorescence from the sample was dispersed by a monochromator (Nikon G-250) and then detected by a microchannel-plate photomultiplier (Hamamatsu, R3809U-52). The instrumental response function (RF) had a full width at half-maximum (fwhm) of ∼60 ps. The observed fluorescence decay was fitted by the convolution of the RF with a multiexponential decay. In the measurements of time-resolved fluorescence spectra, the fluorescence decay was monitored as a function of fluorescence wavelength, and time-resolved fluorescence spectra were obtained by combining the decays at different wavelengths. The output wavelength of the monochromator was scanned under computer control. HeLa cells prepared as described above were gathered into a cuvette with 1 mm optical path, which was used as a population of HeLa cells. The number of a population of HeLa cells was qualitatively estimated to be 10^4−10^8 on the assumption that the volume of a HeLa cell was 3×10^3 μm^3 and cells were tightly packed after the complete precipitation on the cuvette bottom.[24]

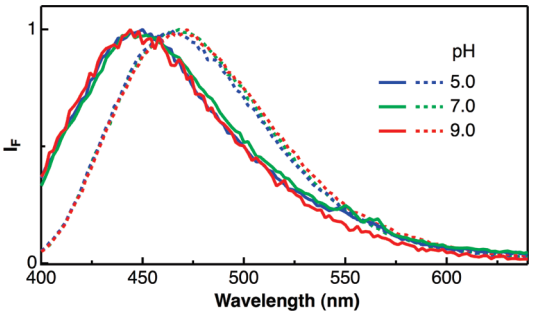

Figure 1. Autofluorescence spectra of HeLa cells (solid lines) and fluorescence spectra of NADH in aqueous solution (dotted lines) at different pH of 5.0 (blue), 7.0 (green), and 9.0 (red) following excitation at 370 nm. The maximum intensity is normalized to unity.

Fluorescence decay profiles of a single cell were obtained using a TCSPC system (Becker&Hickel GmbH, SPC-830) combined with the confocal scanning microscope (Nikon, Digital Eclipse C1). The second harmonic of the mode-locked Ti:sapphire laser (Spectra Physics, Tsunami) was used for excitation. Fluorescence from the single cell was passed through an interference filter and was detected by the above-mentioned microchannel-plate photomultiplier. The pixel dwell time was 13.6 μs at each pixel of the image, and the total scanning number was 3500 for each decay measurement.

3. RESULTS AND DISCUSSION

Figure 1 shows autofluorescence spectra of HeLa cells with intracellular pH of 5.0, 7.0, and 9.0. The excitation wavelength was selected to 370 nm to effectively excite NADH in cells.[1−7,25] Fluorescence spectra of NADH in aqueous solution are also shown for comparison. The fluorescence spectra of NADH both in HeLa cells and in aqueous solution were almost independent of pH. However, it should be noted that the fluorescence spectra of NADH in HeLa cells exhibit a blue shift from those in aqueous solution. The magnitude of the shift is more than 10 nm, which arises from the spectral change upon binding of NADH to proteins.[26,27]

We measured fluorescence decay profiles of NADH in a single HeLa cell under different pH conditions using the TCSPC method and the confocal microscope (Figure 2). The excitation wavelength was 370 nm, and the detected autofluorescence wavelength was 440 nm, which is attributed to NADH in a HeLa cell (Figure 1). In this measurement, the intensity image was obtained for the 256 × 256 pixels from the intensity integration of the fluorescence decay at each pixel, since the fluorescence from each cell was very weak. Then the decay measurements were focused to the central part of a single cell using a clock function of the scanning microscope. Figure S1 in the Supporting Information shows the area inside the single cell for which the decay profiles were measured. The decay profiles measured at all the pixels in this area were accumulated. The average fluorescence lifetime (τ_{av}^{AF}), defined as $\int I_f(t)\,dt/I_f(t=0)$, where $I_f(t)$ is the fluorescence intensity at time t, was determined to be 1.59, 1.44, 1.25, 1.00, and 0.83 ns at intracellular pH 4.5, 5.5, 7.0, 9.0 and 10.0, respectively. This result clearly indicates that the average fluorescence lifetime of NADH in a cell depends on the intracellular pH; τ_{av}^{AF} becomes shorter monotonically, as the intracellular pH increases.

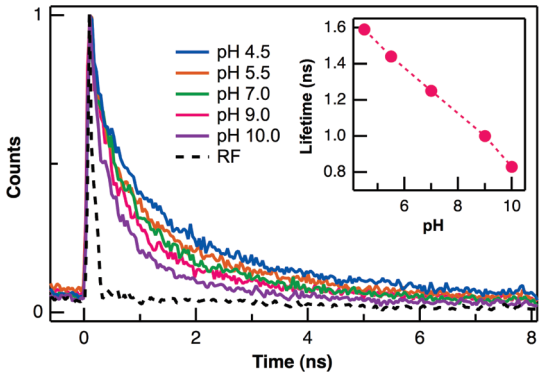

Figure 2. Decay profiles of autofluorescence of a single HeLa cell at different pH. Excitation and detection wavelengths were 370 and 440 nm, respectively. The response function (RF) obtained by monitoring the scattered light under the same experimental condition is also shown by a broken line. The maximum intensity at each decay curve is normalized to unity. Plots of the average fluorescence lifetime as a function of pH are shown in the insert.

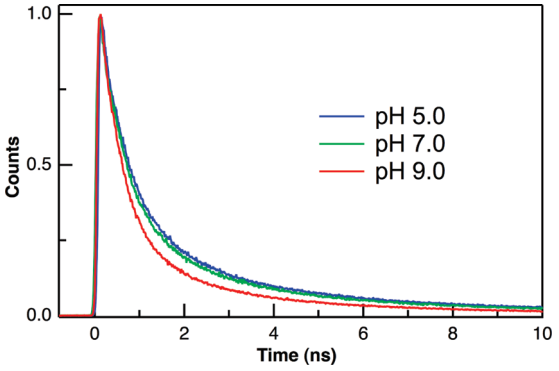

Figure 3. Representative decay profiles of autofluorescence of a population of HeLa cells at different intracellular pH of 5.0, 7.0, and 9.0. Excitation and detection wavelengths were 370 and 440 nm, respectively. The maximum intensity at each decay curve is normalized to unity.

Bulk measurements of autofluorescence decay profiles of a HeLa cell population were also carried out with intracellular pH of 5.0, 7.0, and 9.0 (Figure 3). Excitation and detection wavelengths were 370 and 440 nm, respectively. The observed decay profiles could be fitted by assuming a triexponential decay, i.e., $\Sigma_i A_i \exp(-t/\tau_i)$, where A_i and τ_i are the preexponential factor and the fluorescence lifetime of the ith component, respectively. The lifetime and preexponential factor of these components are shown in Table 1. The lifetime of the fast decaying component was ca. 500 ps, while that of the slow component was ca. 3 ns. Another component whose lifetime was longer than 10 ns was confirmed, although its preexponential factor was ca. 2%. The τ_{av}^{AF} value of a population of HeLa cells is the same as that obtained from a single cell within the experimental uncertainty. The decay profiles could be analyzed by assuming that the lifetime of each decaying component depends on pH; the fluorescence lifetime of every component becomes shorter with increasing intracellular pH (Table 1). These results lead us to a conclusion that the fluorescence of NADH in HeLa cells exhibits significant pH dependence for τ_{av}^{AF}, while the shape of the fluorescence spectrum remains unchanged with pH.

Fluorescence decay profiles of NADH in aqueous solution with medium pH of 5.0, 7.0, and 9.0 are shown in Figure 4. The

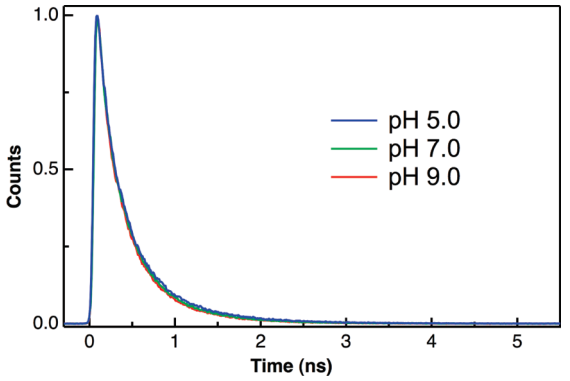

Figure 4. Representative fluorescence decay profiles of NADH in aqueous solution at different pH of 5.0, 7.0, and 9.0. Excitation and detection wavelengths were 370 and 450 nm, respectively. The maximum intensity at each decay curve is normalized to unity.

excitation and fluorescence wavelengths were 370 and 450 nm, respectively. The decay profiles of NADH in aqueous solution could be fitted by assuming a triexponential decay, and the obtained lifetime and preexponential factor are shown in Table 2. Two decaying components in the picosecond time range were dominant at each pH;[28,29] however, it was necessary to consider the component having a lifetime of ca. 1 ns to reproduce the decay in the time range longer than 2 ns, although its preexponential factor was ca. 2%. It is noted that the magnitude of the pH-induced change in τ_{av}^{AF} is markedly smaller in aqueous solution than in HeLa cells; the magnitude of the reduction of τ_{av}^{AF} from pH 5.0 to 9.0 was ca. 30% in cells and that was ca. 10% in aqueous solution, indicating that the interaction between NADH and proteins is a significant factor for the large pH-induced change in τ_{av}^{AF} in cells. The fact that the pH dependence of the fluorescence lifetime of NADH in aqueous solution is small may have prevented so far the detailed investigation of the pH dependence of the NADH fluorescence in cells.

Fluorescence lifetime images of HeLa cells at different intracellular pH ranging from 4.0 to 10.0 were measured using the time-gated detection method with four time-windows,[15−17]

Table 1. Lifetime and Preexponential Factor of Each of Triexponential Decay Components of Autofluorescence of a Population of HeLa Cells at Different pH[a]

pH	av lifetime[b] (ns)	τ_I (ns)	τ_{II} (ns)	τ_{III} (ns)
5.0	1.77 ± 0.20	0.61 ± 0.15 (0.73)	3.30 ± 0.20 (0.24)	17.7 ± 1.8 (0.03)
7.0	1.48 ± 0.20	0.53 ± 0.10 (0.73)	3.10 ± 0.20 (0.25)	15.9 ± 1.6 (0.02)
9.0	1.16 ± 0.20	0.49 ± 0.10 (0.80)	2.75 ± 0.20 (0.18)	13.7 ± 1.4 (0.02)

[a] The preexponential factor of each component is given in parentheses. [b] The average lifetime is given by $\Sigma A_i\tau_i$ (i = I−III).

dx.doi.org/10.1021/jp2058904 |J. Phys. Chem. B 2011, 115, 10385–10390

Table 2. Lifetime and Preexponential Factor of Each of Triexponential Decay Components of Fluorescence of NADH in Aqueous Solution at Different pH[a]

pH	av lifetime[b] (ps)	τ_I (ps)	τ_{II} (ps)	τ_{III} (ns)
5.0	290 ± 20	145 ± 10 (0.61)	470 ± 30 (0.36)	1.1 ± 0.1 (0.03)
7.0	276 ± 20	140 ± 10 (0.60)	430 ± 30 (0.37)	1.1 ± 0.1 (0.03)
9.0	258 ± 20	144 ± 10 (0.66)	440 ± 30 (0.32)	1.1 ± 0.2 (0.02)

[a] The preexponential factor of each component is given in parentheses. [b] The average lifetime is given by $\Sigma A_i\tau_i$ (i = I−III).

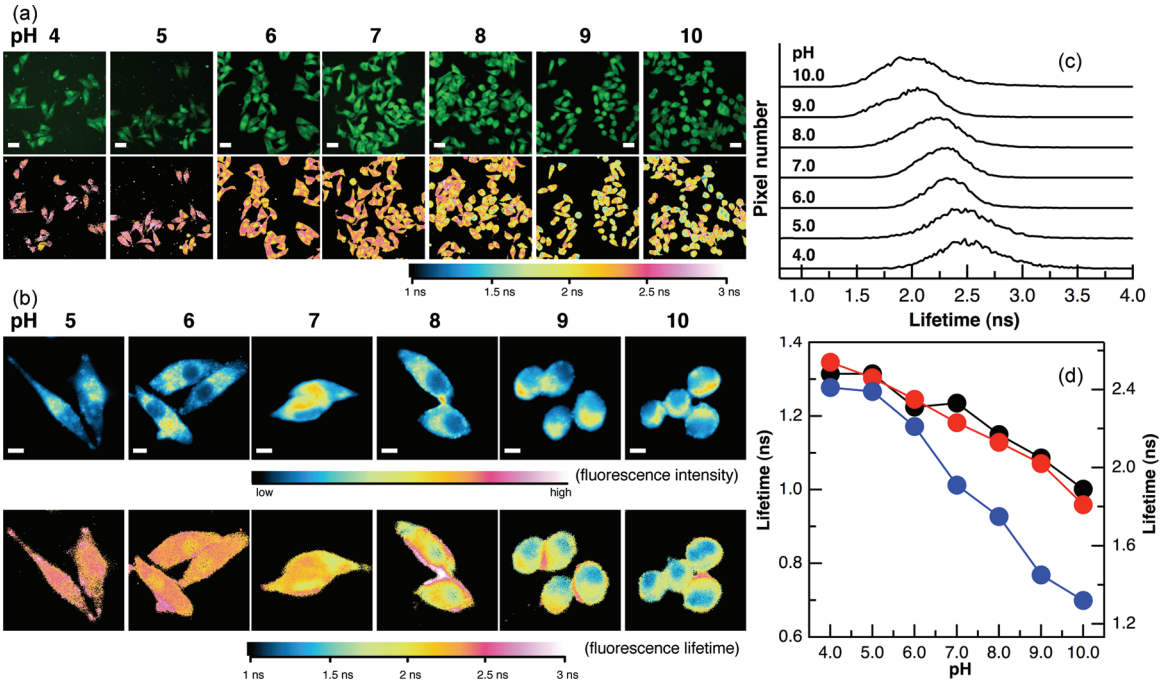

Figure 5. (a) Fluorescence intensity images (upper) and corresponding fluorescence lifetime images (lower) of the autofluorescence of HeLa cells at the intracellular pH indicated at the top. (b) High-resolution images of the fluorescence intensity (upper) and fluorescence lifetime (lower) of a few typical HeLa cells at the indicated intracellular pH. Pseudocolor is also used for the intensity images to show the clear location dependence of the fluorescence intensity. The scale bar is 40 μm in a and 10 μm in b. (c) pH dependence of the histogram of the fluorescence lifetime obtained from the whole area of the fluorescence lifetime images in a. (d) Plots of the fluorescence lifetime as a function of pH using the values obtained from the peak of the histogram of the fluorescence lifetime shown in c (black circles) and those obtained at the bright mitochondria (red circles) and at the dull nuclei (blue circles) of the lifetime images shown in b. The axis at right corresponds to the fluorescence lifetime obtained by the FLIM measurements, while the axis at left corresponds to the corrected values of the lifetime.

and the obtained lifetime images are shown in Figure 5a, together with the corresponding intensity images. The fluorescence lifetime in each pixel of the image was evaluated by analyzing the four time-gated photon signals by assuming a single exponential decay, and the results were converted into a fluorescence lifetime image. Excitation wavelength was 370 nm, and autofluorescence in the region of 417−477 nm was detected. The pseudocolor of the fluorescence lifetime images depends remarkably on pH, confirming that intracellular pH of a cell can be evaluated by FLIM of NADH. The peak of the histogram of the fluorescence lifetime obtained from the whole area of the image, i.e., the distribution of the fluorescence lifetime, becomes shorter as the intracellular pH increases (Figure 5c), which is in agreement with the results of the fluorescence decays.

The lifetime calculated from these fluorescence lifetime images is longer than that determined by the fluorescence decay profiles (Figures 2 and 3) at each pH, which is due to the fact that a part of the fast-decaying portion following photoexcitation was cut in the FLIM measurements to exclude scattered light, and the signal integration at the first window was made from 1 ns after photoexcitation. In fact, the decay profiles in Figure 2 gave the average fluorescence lifetime of 2.17, 1.84, 1.76, 1.71, and 1.55 ns at pH of 4.5, 5.5, 7.0, 9.0 and 10.0, respectively, when the analysis was made using decay profiles in which the first 1 ns part following excitation was cut. Note that the fluorescence of NADH in HeLa cells showed a multiexponential decay (Figure 3 and Table 1).

It is also found that the autofluorescence lifetime of NADH inside a cell is not uniform in highly space-resolved FLIM (Figure 5b), which confirms that τ_{av}^{AF} of NADH depends on the location in a cell. Cell morphology and organelle information are seen in the intensity images. The size of each cellular compartment of a HeLa cell is typical among mammalian cells,[30] and the dull round region with a diameter of ca. 10 μm and the bright region inside a cell with a diameter of 5−10 μm are assigned to a nucleus and mitochondria, respectively. The elongated shape of cells comes from attachment and spreading of cells on culture dishes, the magnitude of which depends on

various factors.[31] Autofluorescence of NADH was brighter in mitochondria than in other areas,[32,33] which may arise from the high concentration of NADH in mitochondria taking part in the electron transport chain to generate ATP. Therefore, the pH dependence of τ_{av}^{AF} obtained by the decay profiles in Figure 2 may be attributed to that of NADH in mitochondria. The values of τ_{av}^{AF} both at nuclei and at mitochondria were evaluated in Figure 5b at each pH, which is shown in Figure 5d. It is found that τ_{av}^{AF} decreases irrespective of the NADH location as the intracellular pH increases. At each pH, the value of τ_{av}^{AF} is smaller in nuclei than in other areas. It is also likely that the magnitude of the pH-induced change is larger in nuclei than in other areas. The difference in the lifetime between nuclei and other areas was also confirmed in the lowly space-resolved FLIM exhibiting many cells at pH ranging from 6 to 10 (Figure 5a). Note that the corrected lifetime is given in Figure 5d, together with the lifetime determined from the fluorescence lifetime images. This correction was made by assuming that the lifetime evaluated from the decay profiles obtained by the TCSPC method is the correct one. The lifetime estimated from the histogram of the FLIM is larger than the average lifetime of the full decay, as mentioned above. It is noted that the fluorescence lifetime of NADH was also reported to be different between nuclei and mitochondria in SiHa cells.[34]

NADH serves as a coenzyme for a variety of dehydrogenase enzymes and is therefore regarded to exist in two forms in living systems, which are referred to as protein-bound and free NADH.[1−8] These two forms are thought to be distinguished by measurements of the fluorescence lifetime because the fluorescence lifetime of the fast decaying component of NADH in living systems is similar to the fluorescence lifetime of NADH in aqueous solution. The slowly decaying component having a nanosecond fluorescence lifetime is assigned to the protein-bound NADH. As mentioned above, the fast and slowly decaying components having fluorescence lifetime of ca. 500 ps and 3 ns, respectively, were confirmed in the decay profiles of NADH in HeLa cells. If the fast and slow components are ascribed to the free and protein-bound NADH, respectively, these two forms should show different fluorescence spectra. This is because the free NADH shows a fluorescence spectrum similar to that of NADH in aqueous solution, which is red-shifted by ca. 10 nm from the spectrum of the protein-bound NADH (Figure 1). As shown in Figure 6, however, the time-resolved autofluorescence spectra of a population of HeLa cells showed that the fast and slowly decaying components exhibited essentially the same fluorescence spectra, and the peak of the fluorescence spectrum in the 0.0−0.2 ns time range (ca. 450 nm) was different from that of the fluorescence spectrum of free NADH in Figure 1 (ca. 460 nm). This result suggests that the observed autofluorescence is due to the protein-bound NADH. One possible explanation for the present multiexponential decay in HeLa cells is that the observed fluorescence mainly arises from NADH bound to different sites on proteins.

NADH interacts with proteins in cells, and protein-bound NADH is predominantly observed in autofluorescence, as already mentioned (Figure 1). The enzyme, with which NADH is bound, may be not unique, but it is unlikely that NADH is bound with different enzymes at different pH, though the interaction between NADH and enzyme may be affected by a change in pH. It is expected that the peak position of the NADH fluorescence shifts, depending on pH, if NADH is bound to different enzymes at different pH. The fact that the autofluorescence spectrum is

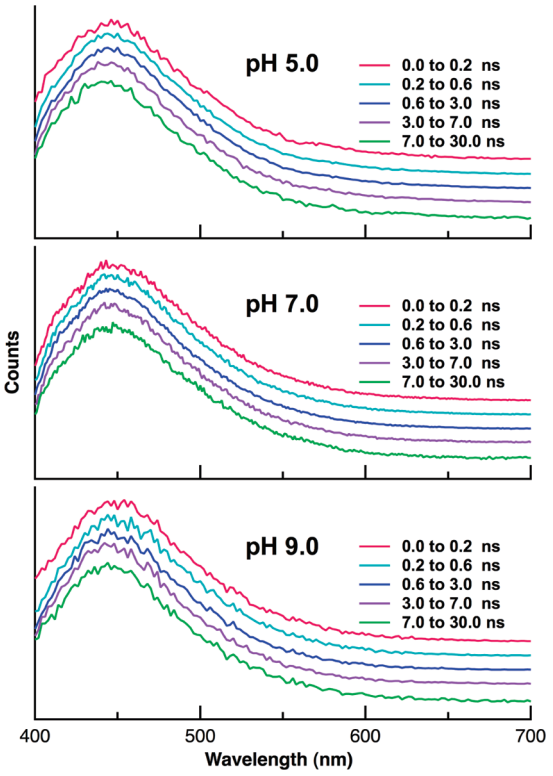

Figure 6. Time-resolved autofluorescence spectra of a population of HeLa cells at different intracellular pH of 5.0, 7.0, and 9.0. Excitation wavelength was 370 nm. The maximum intensity at each spectrum is normalized to unity.

independent of pH and that the pH dependence of the lifetime of NADH in buffer solution is very small suggests that the pH dependence of the autofluorescence of NADH does not come from the pH dependence of the NADH itself, but comes from the pH dependence of the enzyme with which NADH is bound. Then it is considered that the pH dependence of the molecular structure and/or electronic structure of the enzyme with which NADH is bound induces a large pH dependence of the nonradiative decay rate at the emitting state of the bound NADH. The present results remind us of the stress-induced change or apoptosis-induced change in the fluorescence lifetime of the enhanced green fluorescent protein (EGFP) expressed in HeLa cells, where electrostatic field surrounding the EGFP fluorophore, i.e., the electric field produced by the protein matrix surrounding the EGFP fluorophore, is expected to induce the change in the nonradiative decay rate at the emitting state of the EGFP fluorophore.[35−37] Then, a large difference of the nonradiative decay rate of the bound NADH at different pH may arise from the presence of large electric fields produced by the bound enzymes, whose strength depends on pH. Charged and polar groups in protein structures have been suggested to produce a strong electric field of 1−80 MV cm^{-1} for embedded molecules,[38−40] and strong electric fields are considered to exist at the amino terminus of an α-helix.[41] Therefore, NADH may be influenced by such an electric field from proteins and other intracellular substances, resulting in the change in its nonradiative decay rate. In fact, significant electric field effects on photoexcitation dynamics have already been confirmed for molecules and molecular systems.[42] The fact that the fluorescence lifetime of NADH is shorter in nuclei than in mitochondria

implies that NADH is more strongly affected by local electric fields produced from intracellular substances in nuclei than in mitochondria.

Long fluorescence lifetimes were evaluated at the periphery in some cells, as is shown in Figure 5b. At pH 9, for example, the average lifetime was ca. 2.0 ns at mitochondria, while that was ca. 2.5 ns at the contact regions of two cells. This nonuniformity of the fluorescence lifetime might arise from interactions between cell membranes and NADH; however, FLIM measurements with a higher spectral resolution are necessary to clarify the detailed mechanism of the long fluorescence lifetime at the periphery of cells.

4. CONCLUSIONS

The autofluorescence lifetime images of the endogenous NADH were observed in HeLa cells with different intracellular pH. The average fluorescence lifetime of NADH becomes shorter monotonically as the intracellular pH increases, indicating pH imaging in a cell using FLIM of NADH. The pH-induced change in the lifetime of NADH autofluorescence is considered to result from the pH dependence of the interaction between NADH and proteins to which it is bound. Autofluorescence lifetime imaging has the potential to become a powerful method for examining an intracellular environment with subcellular resolution without dye labeling. The present results demonstrate the sensing and monitoring of the spatial distribution of intracellular pH using the fluorescence lifetime of endogenous NADH in living systems.

■ ASSOCIATED CONTENT

Supporting Information. Figure showing the area (square) for which the scanning was done to measure the decay profiles in Figure 2. This material is available free of charge via the Internet at http://pubs.acs.org.

■ AUTHOR INFORMATION

Corresponding Author

*E-mail: nohta@es.hokudai.ac.jp. Phone: +81-11-706-9410. Fax: +81-11-706-9406.

■ ACKNOWLEDGMENT

S.O. and T.A. thank Drs. M. Naya, T. Kasamatsu, and T. Nakatani of FUJIFILM Co. for their great support and fruitful discussion.

■ REFERENCES

(1) Richards-Kortum, R.; Sevick-Muraca, E. *Annu. Rev. Phys. Chem.* **1996**, *47*, 555–606.
(2) Huang, S.; Heikal, A. A.; Webb, W. W. *Biophys. J.* **2002**, *82*, 2811–2825.
(3) Niesner, R.; Peker, B.; Schlüsche, P.; Gericke, K.-H. *ChemPhysChem* **2004**, *5*, 1141–1149.
(4) Skala, M. C.; Riching, K. M.; Gendron-Fitzpatrick, A.; Eickhoff, J.; Eliceiri, K. W.; White, J. G.; Ramanujam, N. *Proc. Natl. Acad. Sci. U. S. A.* **2007**, *104*, 19494–19499.
(5) Ghukasyan, V. V.; Kao, F.-J. *J. Phys. Chem. C* **2009**, *113*, 11532–11540.
(6) Chorvat, D., Jr.; Chorvatova, A. *Laser Phys. Lett.* **2009**, *6*, 175–193.
(7) Berezin, M. Y.; Achilefu, S. *Chem. Rev.* **2010**, *110*, 2641–2684.
(8) Lakowicz, J. R.; Szmacinski, H.; Nowaczyk, K.; Johnson, M. L. *Proc. Nati. Acad. Sci. U. S. A.* **1992**, *89*, 1271–1275.
(9) Iweibo, I. *Biochim. Biophys. Acta* **1976**, *446*, 192–205.
(10) Paradiso, A. M.; Tsien, R. Y.; Machen, T. E. *Nature* **1987**, *325*, 447–450.
(11) Yamashiro, D. J.; Maxfield, F. R. *Trends Pharmacol. Sci.* **1988**, *9*, 190–193.
(12) Wallrabe, H.; Periasamy, A. *Curr. Opin. Biotechnol.* **2005**, *16*, 19–27.
(13) Becker, W.; Bergmann, A.; Biskup, C. *Microsc. Res. Tech.* **2007**, *70*, 403–409.
(14) Levitt, J. A.; Matthews, D. R.; Ameer-Beg, S. M.; Suhling, K. *Curr. Opin. Biotechnol.* **2009**, *20*, 28–36.
(15) Gerritsen, H. C.; Asselbergs, M. A. H.; Agronskaia, A. V.; van Sark, W. G. J. H. M. *J. Microsc.* **2002**, *206*, 218–224.
(16) Wang, H. P.; Nakabayashi, T.; Tsujimoto, K.; Miyauchi, S.; Kamo, N.; Ohta, N. *Chem. Phys. Lett.* **2007**, *442*, 441–444.
(17) Ohta, N.; Nakabayashi, T.; Nagao, I.; Kinjo, M.; Aoki, Y.; Tanaka, M. *Proc. SPIE* **2009**, *7190*, 71900R-1–71900R-11.
(18) Thomas, J. A.; Buchsbaum, R. N.; Zimniak, A.; Racker, E. *Biochemistry* **1979**, *18*, 2210–2218.
(19) Nedergaard, M.; Desai, S.; Pulsinelli, W. *Anal. Biochem.* **1990**, *187*, 109–114.
(20) Sanders, R.; Draaijer, A.; Gerritsen, H. C.; Houpt, P. M.; Levine, Y. K. *Anal. Biochem.* **1995**, *227*, 302–308.
(21) Robey, R. B.; Ruiz, O.; Santos, A. V. P.; Ma, J.; Kear, F.; Wang, L.-J.; Li, C.-J.; Bernardo, A. A.; Arruda, J. A. L. *Biochemistry* **1998**, *37*, 9894–9901.
(22) Tafani, M.; Cohn, J. A.; Karpinich, N. O.; Rothman, R. J.; Russo, M. A.; Farber, J. L. *J. Biol. Chem.* **2002**, *277*, 49569–49576.
(23) Tsushima, M.; Ohta, N. *J. Chem. Phys.* **2004**, *120*, 6238–6245.
(24) Zhao, L.; Kroenke, C. D.; Song, J.; Piwnica-Worms, D.; Ackerman, J. J. H.; Neil, J. J. *NMR Biomed.* **2008**, *21*, 159–164.
(25) Schweitzer, D.; Schenke, S.; Hammer, M.; Schweitzer, F.; Jentsch, S.; Birckner, E.; Becker, W.; Bergmann, A. *Microsc. Res. Tech.* **2007**, *70*, 410–419.
(26) Brochon, J.-C.; Wahl, P.; Monneuse-Doublet, M.-O.; Olomucki, A. *Biochemistry* **1977**, *16*, 4594–4599.
(27) König, K.; Berns, M. W.; Tromberg, B. J. *J. Photochem. Photobiol., B* **1997**, *37*, 91–95.
(28) Evans, N. D.; Gnudi, L.; Rolinski, O. J.; Birch, D. J. S.; Pickup, J. C. *J. Photochem. Photobiol., B* **2005**, *80*, 122–129.
(29) Zelent, B.; Troxler, T.; Vanderkooi, J. M. *J. Fluoresc.* **2007**, *17*, 37–42.
(30) Tomosugi, W.; Matsuda, T.; Tani, T.; Nemoto, T.; Kotera, I.; Saito, K.; Horikawa, K.; Nagai, T. *Nat. Methods* **2009**, *6*, 351–353.
(31) Taylor, A. C. *Exp. Cell Res.* **1961**, Suppl. 8, 154–173.
(32) Sud, D.; Zhong, W.; Beer, D. G.; Mycek, M.-A. *Opt. Express* **2006**, *14*, 4412–4426.
(33) Niesner, R. A.; Andresen, V.; Gunzer, M. *Immunol. Rev.* **2008**, *221*, 7–25.
(34) Li, D.; Zheng, W.; Qu, J.-Y. *Opt. Lett.* **2008**, *15*, 2365–2367.
(35) Nakabayashi, T.; Nagao, I.; Kinjo, M.; Aoki, Y.; Tanaka, M.; Ohta, N. *Photochem, Photobiol. Sci.* **2008**, *7*, 671–674.
(36) Ito, T.; Oshita, S.; Nakabayashi, T.; Sun, F.; Kinjo, M.; Ohta, N. *Photochem. Photobiol. Sci.* **2009**, *8*, 763–767.
(37) Nakabayashi, T.; Kinjo, M.; Ohta, N. *Chem, Phys. Lett.* **2008**, *457*, 408–412.
(38) Callis, P. R.; Burgess, B. K. *J. Phys. Chem. B* **1997**, *101*, 9429–9432.
(39) Park, E. S.; Andrews, S. S.; Hu, R. B.; Boxer, S. G. *J. Phys. Chem. B* **1999**, *103*, 9813–9817.
(40) Kriegl, J. M.; Nienhaus, K.; Deng, P.; Fuchs, J.; Nienhaus, G. U. *Proc. Natl. Acad. Sci. U. S. A.* **2003**, *100*, 7069–7074.
(41) Lockhart, D. J.; Kim, P. S. *Science* **1992**, *257*, 947–951.
(42) Ohta, N. *Bull. Chem. Soc. Jpn.* **2002**, *75*, 1637–1655.